GIS-Based Mapping of Geotechnical and Geophysical Properties of Lahore Soils

Muhammad Daniyal (daniaslam2@gmail.com)
University of Engineering and Technology Lahore
Ghulam Mohyuddin Sohail
University of Engineering and Technology Lahore
Hafiz Muhammad Awais Rashid
University of Engineering and Technology Lahore

Research Article

Keywords: IDW, Kriging, SPT, GIS, Soil characterization

Posted Date: August 19th, 2022

DOI: https://doi.org/10.21203/rs.3.rs-1963057/v1

Additional Declarations: No competing interests reported.

Version of Record: A version of this preprint was published at Environmental Earth Sciences on October 31st, 2023. See the published version at https://doi.org/10.1007/s12665-023-11201-w.

Abstract

The spatial distribution of geotechnical and geophysical properties of soil delineates the subsurface soil type and condition necessary to ensure structural safety and serviceability, detailed investigations for engineering projects, and the foundation design under static and seismic loading conditions. This study presents the spatial distribution of soil type, standard penetration test (SPT) N values, bearing capacity, groundwater depth, and shear wave velocity using the database from sixty-five boreholes in GIS (geographical information system) software. The data were processed and interpreted through geostatistical contouring techniques (e.g., kriging and inverse distance weightage). The cross-plots were generated further to facilitate the interpretation of contour maps at unsampled locations. A correlation was established between measured and estimated shear wave velocity and standard penetration test N-values for the study area. It was then tested against the literature-based correlations to enhance the reliability of predicted geotechnical properties. A correlation coefficient of 0.77 between measured and predicted SPT N values improves the reliability of estimated properties (e.g., bearing capacity, shear wave velocity) at unsampled locations. The SPT N values, shear wave velocity, and allowable bearing capacity seem to be interdependent and varied with soil type and may be used for soil characterization and shallow foundation design at undrilled locations. The geotechnical maps generated in this study for Lahore city are novel and consistent with the soil types of the study area. Geotechnical engineers can use these maps for preparing geotechnical reports for the study area.

Introduction

Subsurface geotechnical information (e.g., engineering and geophysical properties of soil) is essential for designing and constructing geotechnical projects (e.g., earth dams, foundations, excavation, embankments, and seismic hazards analysis). Geotechnical properties (e.g., N value from the standard penetration test (SPT), bearing capacity, shear modulus, permeability, stiffness, and strength) are affected by the size, shape, microscopic structure, and arrangement of soil particles (Sharma & Rahman, 2016). These properties can be determined through drilling boreholes and geophysical surveys; however, this data covered a limited surface and subsurface area. Moreover, getting the data of a large area using drilling and geophysical methods involves a high cost. Most of the time, geotechnical engineers rely on the limited available data and try to interpolate between boreholes, which generates a need to explore different interpolation techniques for knowing the spatial distribution of geotechnical properties.

Soil classification, SPT N-value, and shear wave velocity are the most significant geotechnical parameters in designing a foundation, computing the allowable bearing capacity (ABC) of the shallow foundation and the axial capacity for both types of foundations (e.g., driven and bored). The properties of cohesive and non-cohesive soils (e.g., consistency and compressive strength of cohesive soils, compactness, relative density, angle of friction for cohesionless soils, shear wave velocity) and allowable bearing capacity of the shallow foundation are estimated from SPT N-value. Multiple empirical relationships have been established between SPT N-value and shear wave velocity because shear wave velocity is the most critical parameter for studying site response against earthquakes. In geotechnical

earthquake engineering, the shear modulus is an important parameter estimated from shear wave velocity and used to determine the dynamic response of the soil. Bandyopadhyay, Sengupta, and Reddy (2021) have conducted site response analysis based on the soil classification, soil resistance parameters, and shear wave velocity for different soils and found that soil type significantly impacts this analysis.

The geographical Information System (GIS) is a valuable tool for capturing, presenting, and analyzing geographically referenced data (Singh, Noor, Chitra, & Gupta, 2018). Geographic Information System provides valuable tools for inputting data into the database, retrieving specific data items for further processing, and software components that can evaluate or manipulate the recovered data to produce desired information in a particular form (Mhaske & Choudhury, 2011). Geotechnical evaluation of an area requires an optimum number of data points to develop a comprehensive surface/subsurface model. GIS can be used for analyzing/mapping a bulk volume of data for geotechnical investigations. In geotechnical practice, GIS is used in four ways: data integration, data visualization and analysis, planning and summarizing site activities, and data presentation (Singh et al., 2018). Due to the fast-growing of engineering technologies, the modern techniques of geography are combined with engineering to form new strategies for data integration. The corrected SPT N-values, soil types, groundwater depth, shear wave velocity, and allowable bearing capacity for shallow foundations are mapped using the Geographic information system through spatial data treatment and management. Kriging and IDW (Inverse distance weight) are the user-friendly techniques available in GIS for mapping the data. However, an evaluation of these geostatistical techniques is necessary to decide the suitability of a specific technique for a certain area.

Lahore has an estimated population of 11.738 million (Desa, 2018), which demands the launch of more infrastructure development projects. Considering the demand for infrastructure developments, conducting detailed subsurface geotechnical investigations is essential. Previously published studies (Khan, Rashid, Israr, & Zhang, 2022; Shafique, Khan, Mustafa, & Arif, 2012) on Lahore focussed on a few parameters and missed several parts of the city, which constrain the applicability of those studies throughout the city. This study collected data from boreholes drilled at different locations in Lahore city, and maps of geotechnical properties were constructed using GIS.

Study Area

Lahore is Pakistan's second largest metropolitan city and the capital city of the province of Punjab. It is also the 18th largest city in the world. It is located at 31°32' 59" N and 74°20' 37" E with a covered area of 1,772 km^2. Lahore city has a very high population growth rate, and its urban growth has increased by 32% in the last 20 years.

Lahore is at an average elevation of 210 meters above mean sea level. Lahore rests on the Bari Doab, which is an alluvial plain. Bari Doab belongs to the Indo-Gangetic alluvial plain, which the Indus River and its tributaries create. This doab consists of Quaternary alluvium, which overlies Metamorphic and igneous rocks of the Precambrian age and semi-consolidated Tertiary rocks (Kadwai & Siraj, 1964). The

alluvial compound of Pleistocene and current age denotes the modern sedimentation in an environment that has its commencement in the Mid-Tertiary periods. This alluvial compound mainly consists of silt, clay, and fine to medium sand (Malik, 2015).

Methodology

The data used in this study were extracted from the geotechnical reports prepared by different companies working in Lahore city. These geotechnical reports were collected with the consent of companies and bear no conflict of interest. The data of sixty-five boreholes (with total depth of 10 m) were selected based on data quality and area coverage. The data was processed through different quality check parameters, e.g., the study of descriptive statistics of data to discard anomalies, making sure that a sufficient number of soil samples were used for laboratory testing for each borehole, confirming the location and sparsity of boreholes through geographical information system (GIS). An example of descriptive statistics for properties at 1m depth is given in Table 1; similar tables were also developed for all depth intervals from 1m to 10m. A workflow used to generate geotechnical maps is shown in Fig. 1.

Table 1
Descriptive statistics for SPT N values, bearing capacity, and shear wave velocity at 1m depth

Properties	SPT N-Value	Bearing Capacity (kPa)	Shear Wave Velocity (m/sec)
Mean	7.35	149.50	155.11
Median	6.00	141.46	149.05
Minimum	1.00	70.73	14.00
Maximum	22.00	364.54	267.28
Range	21.00	293.81	253.28
Standard deviation	4.12	56.31	48.34
Coefficient of variation (%)	55.99	37.67	31.16

The following parameters were extracted from selected borehole records:

1. Soil Classification
2. SPT N values
3. Shear wave velocity
4. Allowable Bearing Capacity (ABC)
5. Groundwater table (GWT)

Table 2
Numerical codes for soil types encountered in the study area

Soil Type	Symbol	Code
Lean Clay	CL	1
Silt	ML	2
silty Clay/clayey Silt	CL-ML	3
silty Sand	SM	4
Poorly Graded Sand with Silt	SP-SM	5

Soil classification was done based on the Unified Soil Classification System (USCS), which classified the soils into coarse-grained and fine-grained soils (ASTM-D2487, 2017; Kalinski, 2011). Different soil types were assigned a code to generate soil type maps, as given in Table 2. The SPT N values at a 1 m depth interval in selected boreholes were studied and corrected to SPT N_{60} before the construction of final maps. The shear wave velocity (V_S) measured in multiple boreholes was used as a reference value to correct estimated Vs. Allowable bearing capacity was computed from SPT N_{60} and mapped. The water table maps were generated and compared to Vs, SPT N-value, and ABC maps. The 2D models and cross-plots of geotechnical properties were developed to discuss their interrelationships.

The satellite image of the study area was obtained from google earth software. This image was uploaded in ArcMap (a module in GIS software) to get a georeferenced map of the study area, as shown in Fig. 2a. Several boreholes were selected from east to west of the study area to develop a subsurface cross-section, as shown by a polygon in Fig. 2a and the subsurface section in Fig. 2b. The numerical codes assigned to each soil type were used to generate relevant maps in GIS. Similarly, the database for SPT N values, Vs, bearing capacity, and water table depth were developed in GIS (e.g., latitude, longitude, serial number, borehole number, depth, relevant property value) for mapping at different depth intervals. Two contouring techniques in ArcMap, Kriging, and IDW, are tested for mapping. Different semi-variogram models (e.g., linear, exponential, logarithmic) available in Kriging were run to optimize the interpolation between two boreholes/points. Maps from Kriging and IDW were compared to decide the best suitable technique for mapping geotechnical properties in the study area, as shown in Fig. 3. In the map of SPT N_{60}, as shown in Fig. 3, the IDW produces a more detailed trend (high resolution) and introduces less value of RMSE (root mean square error) compared to Kriging, so IDW was used for generating all other maps in this study.

Results And Discussion

Soil Classification

The soil was classified using the USCS soil classification system. The numeric codes were assigned to each type of soil for mapping, as given in Table 1. The CL and ML groups are dominant at 1m and 2m depth intervals, respectively, as shown in Figs. 4A and 4B. Soil belonging to the CL-ML group is also located at a few spots in the center and south-center of the study area at 1m and 2 m depth intervals. It can be seen from Figs. 4C and 4D that most of the soil belongs to the CL-ML group at 3m and 4m depth intervals. There are a few spots in the south-center and southeast of the study area where the soil belongs to the ML group, as shown in Figs. 4C and 4D. Soil belonging to the SM group is also located at a few spots in the north-center and center of Lahore city, at 3m and 4 m depth intervals. The maps for other depth intervals are given in the Appendix, showing the dominancy of silty sand, sandy silt, and poorly graded sand with silty soils from 5m to 10m depth intervals consistent with subsurface cross-section, as shown in Fig. 2b.

SPT N-values

The SPT N-Values were mapped to assess the soil-resistance index and relate to other geotechnical properties (e.g., shear wave velocity, allowable bearing capacity). Figure 5 shows the maps of SPT N-values at 1m, 2m, 3m, and 4m depth intervals. These maps show the increase in N-value with depth in the northeast of Lahore city. The SPT N-values (field blows) at 1m and 2m depth, as shown in Figs. 5A and 5B, show similar trends. The minimum range of SPT N-values (1–4) is located at the center of Lahore, with some higher values (7–8) at a few locations. It is because of the presence of the very soft unconsolidated clay layer. The N-Values gradually increase from center to northwest as the soil type changes from clay to silt. The maximum SPT N-Values (13–18) are located at a few spots in the southeast of Lahore city, as shown in Fig. 5D. The N values at 4m depth (Fig. 5D) are higher at the center of Lahore than in the northwest and southeast of the study area, as the soil type at the center of Lahore at 4 m depth is purely silt, while in the northwest and southeast, the soil type is silty clay/clayey silt.

Data of some boreholes are not used for mapping to cross-validate the generated maps. Figure 6 shows the graph between observed SPT N-values (measured in boreholes and not used in mapping) and predicted SPT N-values (extracted from the map at the same location where the SPT test was run). The coefficient of determination (R^2 = 0.77) is in an acceptable range. Thus, it shows a positive correlation between Vs and SPT-N values, and the overestimated and underestimated values fall within 20% of the trend line.

The SPT N-values were further corrected to obtain SPT N60 values. IDW was used to map corrected SPT N60 values, and these maps show a similar trend compared to SPT N values in all parts of the study area. A cross plot of the SPT N-value and SPT N60 from 1m to 10m depth intervals, as shown in Fig. 7, shows different linear trends fitted to the corrected blows with depth. For shallow depth intervals (1–4 m), N60 (corrected blows) should be calculated using Eq. 1. For the deeper depth intervals (> 4 m), the coefficient of 0.56 should be increased by 10%, as shown in Fig. 7.

$$N_{60} = 0.56N \quad \text{.....1}$$

Shear Wave Velocity

The measured shear wave velocity (Vs) and SPT N-values of the same boreholes are cross-plotted, as shown in Fig. 8, which shows the shear wave velocity increased with SPT N-values and depth. The plotted data followed a power trend line which produced a relationship between Vs and SPT N-values, as given in Eq. 2. Further, this Eq. (2) is evaluated against literature-based equations, as provided in Table 3 and plotted in Fig. 9.

$$Vs = 89.01N^{0.35} \quad \text{.....2}$$

Table 3
Compilation of empirical equations for the estimation of Vs using SPT-N values

Serial No.	Relationship	Soils	Sources
1	$Vs = 82.60 * N^{0.430}$	ALL	Hanumantharao and Ramana (2008)
2	$Vs = 84.00 * N^{0.310}$		Ohba and Toriumi (1970)
3	$Vs = 91.00 * N^{0.340}$		Imai (1977)
4	$Vs = 85.35 * N^{0.348}$		Ohta and Goto (1978)
5	$Vs = 121.00 * N^{0.270}$		Yokota et al. (1991)
6	$Vs = 61.00 * N^{0.500}$		Seed and Idriss (1981)
7	$Vs = 107.60 * N^{0.360}$		Athanasopoulos (1970)
8	$Vs = 90.00 * N^{0.309}$		Hasancebi and Ulusay (2007)
9	$Vs = 95.64 * N^{0.301}$		Maheswari et al. (2010)

Based on Eq. 2 and relationships mentioned in Table 2, the Vs is estimated using the SPT N value. A cross plot between calculated Vs and SPT N value, as shown in Fig. 9, depicts the coefficient of determination (R^2) as 1, and most of the points are concentrated in the middle near to points generated by Eq. 2, which enhances the confidence in the derived relationship in this study. Some literature-based relations overestimate (about 25% higher than Vs estimated by Eq. 2) or underestimate (about 20% lower than Vs estimated by Eq. 2) the Vs, as shown in Fig. 9. However, the R^2 is 1 for both estimations.

Shear wave velocity (Vs) is estimated at two depth intervals (1m to 6m and 7m to 10m) in all available boreholes using Eq. 2. The obtained data is interpolated using the IDW technique to generate the maps, as shown in Fig. 10. The shear wave velocity for the 1m to 6m layer is lower at the north-center of Lahore compared to the southeast; as shown in Fig. 10A, it also follows the smaller N-values encountered in this area, as previously shown in Fig. 5. The maximum shear wave velocity for the 1–6 m layer is located at a few spots in the northeast of the study area. The shear wave velocity for the 7–10 m layer is higher at the center of Lahore than in the southeast of the study area, as depicted in Fig. 10B, and follows the recording of higher N-values at the center than in the southeast of the study area.

In Fig. 10A, the encircled zones represent the area where the root mean square error (RMSE = $\sqrt{\frac{1}{n}\sum_{i=1}^{n}(predicted - observed)^2}$) between measured (or observed) and predicted (extracted from the map) Vs is calculated, as given in Table 4. There is a significant error in the predicted Vs, which may be due to the exclusion of other factors in the prediction of Vs, e.g., void ratio, saturation, and mineralogy. The proposed relationship (Eq. 2) overestimates the Vs at a few undrilled locations and must be corrected through soil physics modeling, which is beyond the scope of this study.

Table 4
Root mean square error (RMSE) of shear wave velocity (Vs) for the top (1m-6m) layer

Locality	Depth	Shear Wave Velocity (m/sec)		RMSE (m/sec)
		Observed	**As predicted from Eq. 2**	
Wagah Town	Top 1–6 m layer	166	214	48.0
Shalamar Town		178	208	30.0
Data Gunj Bukhsh Town		181	202	21.0
Gulberg Town		217	202	15.0
Samanabad Town		270	190	80.0

Bearing Capacity

Bearing capacity is evaluated for the shallow square foundation of 1m x 1m size and IDW was applied to bearing capacity data for mapping. Figure 11 shows the bearing capacity variation in different Lahore city zones. The bearing capacity at 1m and 2m depth, as shown in Figs. 11A and 11B, are leading the same trends. The minimum range of bearing capacity is located at the north-center and south-center of Lahore city; this is also supported by the lower N-values at these locations, as the bearing capacity is calculated using corrected N-values. The bearing capacity gradually increases from the center to the east and west of the study area, with some abruptions of lower values at a few locations. The maximum bearing capacity is located near to southeast area (Cantonment Area) of Lahore city, as shown in Figs. 11A and 11B, which is consistent with higher N-values in this area. The groundwater table is at a very deep (> 30m depth) in this area which has no impact on bearing capacity values.

The data of 40 boreholes are utilized to generate 2D models and assess the lateral and vertical variations, as shown in Fig. 12. Points A, B, and C are the same boreholes used for the cross-section shown in Fig. 2. At deeper depth intervals (> 5m) the SPT N-values and Vs vary significantly compared to at shallow depth intervals (< 5m), which may be due to the dominancy of poorly graded silty sands at deeper depth intervals.

The SPT N-values, Vs, and bearing capacity are cross-plotted, as shown in Fig. 13. The plot shows three different zones (colors) in which the plotted properties positively correlate. The thickness and geometrical shape of these zones are not uniform, highlighting different boundary values for each zone due to the change in depth and soil type. Figures 12 and 13 show that the soil type varies laterally and vertically, consistent with the subsurface soil cross-section and contour maps as shown in Figs. 2b and 4, respectively. These plots can predict soil types at undrilled locations, saving drilling costs for new boreholes in the study area. Figure 13 is helpful for geotechnical engineers in foundation design, as they can choose the value of bearing capacity based on encountered SPT N-value. Similarly, shear wave velocity can also be noted from this figure and can be used in earthquake design evaluations.

Groundwater Table

The depth of the groundwater table was extracted from borehole logs. It was interpolated and mapped. Figure 14 shows the variation in groundwater table in the study area. The shallowest depth of groundwater table (~ 5m) was located in the south-center of Lahore city. In contrast, the center and north-center of the study area had the highest groundwater table depth (~ 35m). The GWT depth gradually increased from the west (~ 11m) to the study area's center (~ 35m). The water table map was consistent with a model of hydraulic heads with reference to water tube wells drilled in the study area. The two cup-shaped depressions at the center of the city were due to the excessive abstraction of water and were also observed previously by (Ahmad et al., 2002). CL soils at the top of the study area can facilitate the groundwater table recharge north of the Ravi River.

Conclusion

This study mapped the SPT N-values, shear wave velocity, bearing capacity, and groundwater table that covered the entire city of Lahore, which may significantly work without further drilling of boreholes. These maps can act as a reference for structural/foundation engineers. These maps were also verified through measured values at several locations through a rigorous statistical analysis, which enhanced the confidence in estimated values at undrilled locations.

The IDW technique for mapping seems most suitable for the study area compared to Kriging. The kriging technique does not produce finer details on the maps than IDW and introduces high RMSE for all geotechnical and geophysical properties.

The measured Vs and SPT-N values were cross-plotted to establish a new relationship to estimate Vs. The estimated values lay with the values calculated from relationships extracted from literature; however,

literature-based relationships overestimate or underestimate the Vs. This issue needs further studies through soil physics models after including all missing parameters (e.g., void ratio, mineralogy, saturation).

Declarations

Funding

The authors declare that no funds, grants, or other support were received during the preparation of this manuscript.

Competing Interests

The authors have no relevant financial or non-financial interests to disclose.

Author Contributions

All authors contributed to the study conception and design. Material preparation, data collection, and analysis were performed by Muhammad Daniyal and Ghulam M. Sohail. The first draft of the manuscript was written by Muhammad Daniyal and H. M. A. Rashid commented on previous versions of the manuscript. All authors read and approved the final manuscript.

References

1. Ahmad, M., Rafiq, M., Akram, W., Tasneem, M., Ahmad, N., Iqbal, N., & Sajjad, M. (2002). Assessment of aquifer system in the city of Lahore, Pakistan using isotopic techniques.
2. ASTM-D2487. (2017). Standard Practice for Classification of Soils for Engineering Purposes (Unified Soil Classification System). In. West Conshohocken, PA.: American Society for Testing and Materials.
3. Athanasopoulos, G. (1970). Empirical correlations Vso-NSPT for soils of Greece: A comparative study of reliability. WIT Transactions on The Built Environment, *15*.
4. Bandyopadhyay, S., Sengupta, A., & Reddy, G. (2021). Development of correlation between SPT-N value and shear wave velocity and estimation of non-linear seismic site effects for soft deposits in Kolkata city. Geomechanics and Geoengineering, *16*(1), 1–19. doi:https://doi.org/10.1080/17486025.2019.1640898
5. Hanumantharao, C., & Ramana, G. (2008). Dynamic soil properties for microzonation of Delhi, India. Journal of earth system science, *117*(2), 719–730. doi:https://doi.org/10.1007/s12040-008-0066-2
6. Hasancebi, N., & Ulusay, R. (2007). Empirical correlations between shear wave velocity and penetration resistance for ground shaking assessments. Bulletin of Engineering Geology & the Environment, *66*(2), 203–213. doi:https://doi.org/10.1007/s10064-006-0063-0
7. Imai, T. (1977). *P and S wave velocities of the ground in Japan.* Paper presented at the Proc. 9th ICSMFE.

8. Jafari, M. K., Shafiee, A., & Razmkhah, A. (2002). Dynamic properties of fine grained soils in south of Tehran. Journal of Seismology Earthquake Engineering, *4*(1), 25–35.
9. Kadwai, S., & Siraj, A. (1964). The Geology of Bari Doab, West Pakistan. *WAPDA Water Soil Investigation Division. Bulletin*(8).
10. Kalinski, M. E. (2011). *Soil mechanics: lab manual*: John Wiley & Sons.
11. Maheswari, R. U., Boominathan, A., & Dodagoudar, G. (2010). Use of surface waves in statistical correlations of shear wave velocity and penetration resistance of Chennai soils. Geotechnical and Geological Engineering, *28*(2), 119–137. doi:https://doi.org/10.1007/s10706-009-9285-9
12. Malik, A. (2015). Geotechnical statistical evaluation of Lahore site data and deep excavation design. Civil and Environmental Engineering Master's Project Reports, *13*.
13. Mhaske, S. Y., & Choudhury, D. (2011). GIS-GPS based map of soil index properties for Mumbai. In *Geo-frontiers 2011: Advances in geotechnical engineering* (pp. 2366–2375).
14. Ohba, S., & Toriumi, I. (1970). *Dynamic response characteristics of Osaka Plain.* Paper presented at the Proceedings of the annual meeting AIJ (in Japanese).
15. Ohta, Y., & Goto, N. (1978). Empirical shear wave velocity equations in terms of characteristic soil indexes. Earthquake engineering structural dynamics, *6*(2), 167–187. doi:https://doi.org/10.1002/eqe.4290060205
16. Seed, H. B., & Idriss, I. (1981). *Evaluation of liquefaction potential sand deposits based on observation of performance in previous earthquakes.* Paper presented at the ASCE national convention (MO).
17. Sharma, B., & Rahman, S. K. (2016). Use of GIS based maps for preliminary assessment of subsoil of Guwahati city. Journal of Geoscience and Environment Protection, *4*(05), 106. doi:https://doi.org/10.4236/gep.2016.45011
18. Singh, A., Noor, S., Chitra, R., & Gupta, M. (2018). Applications of GIS in Geotechnical Engineering: Some Case Studies. International Journal of Scientific Engineering and Science, *2*(3), 34–38.

Figures

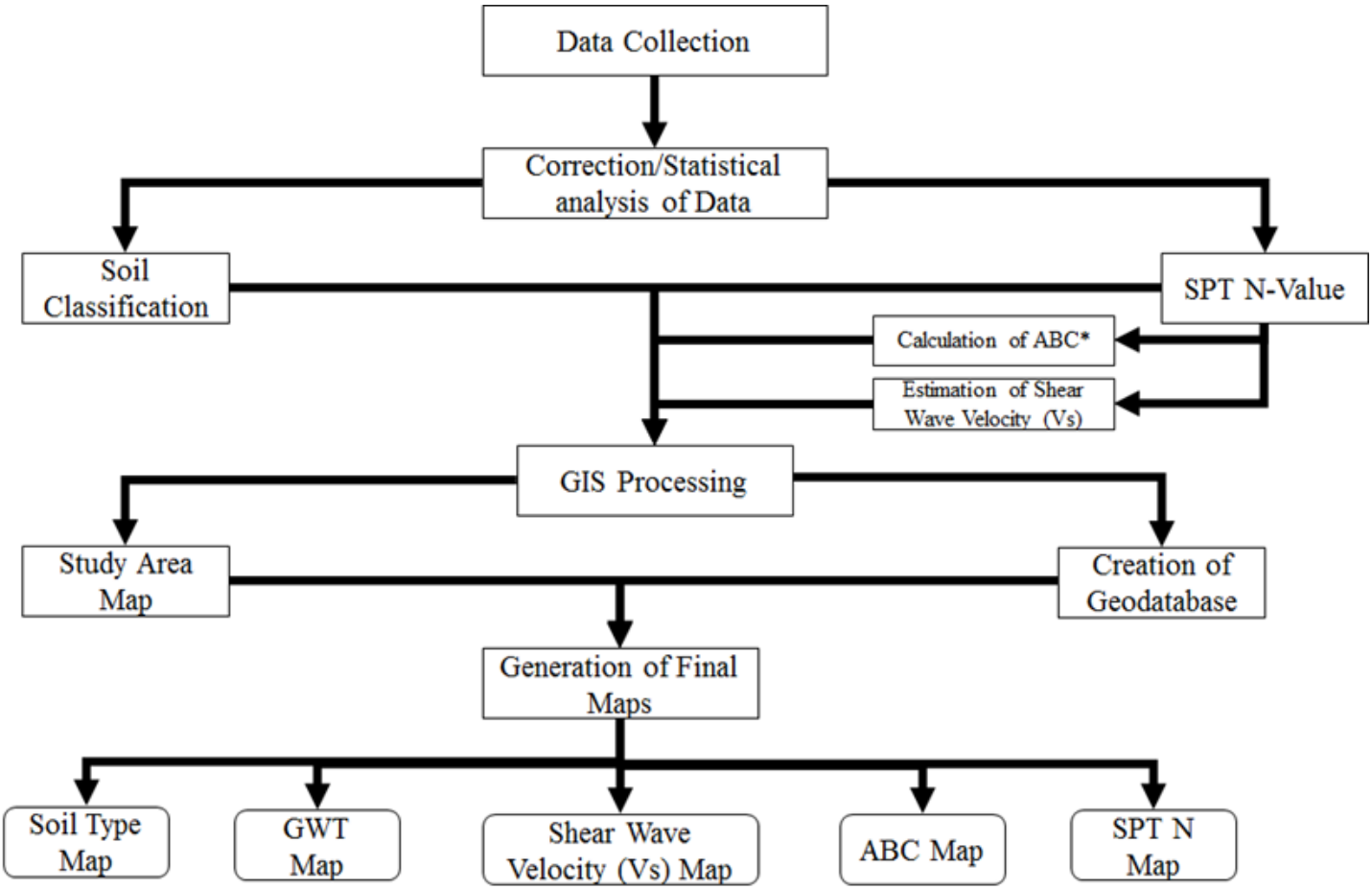

Figure 1

Flowchart shows steps of the methodology

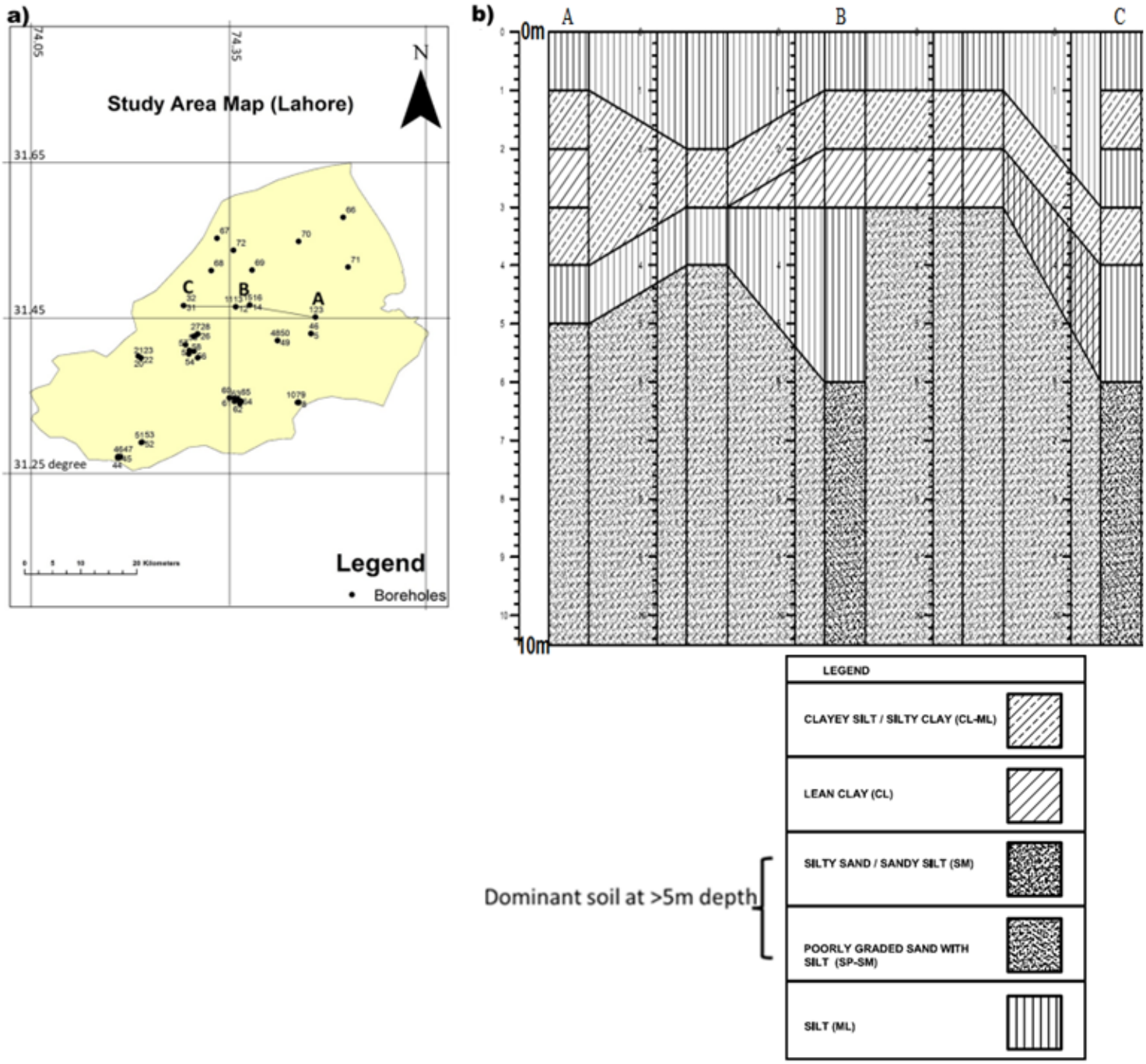

Figure 2

(a) Georeferenced map of Lahore with the location of boreholes, a polyline is connecting boreholes at A, B, and C points (b) Subsurface soil cross-section along the polyline drawn in part a of this figure, the bracket in legend represents the dominant soil encountered at a depth greater than 5m

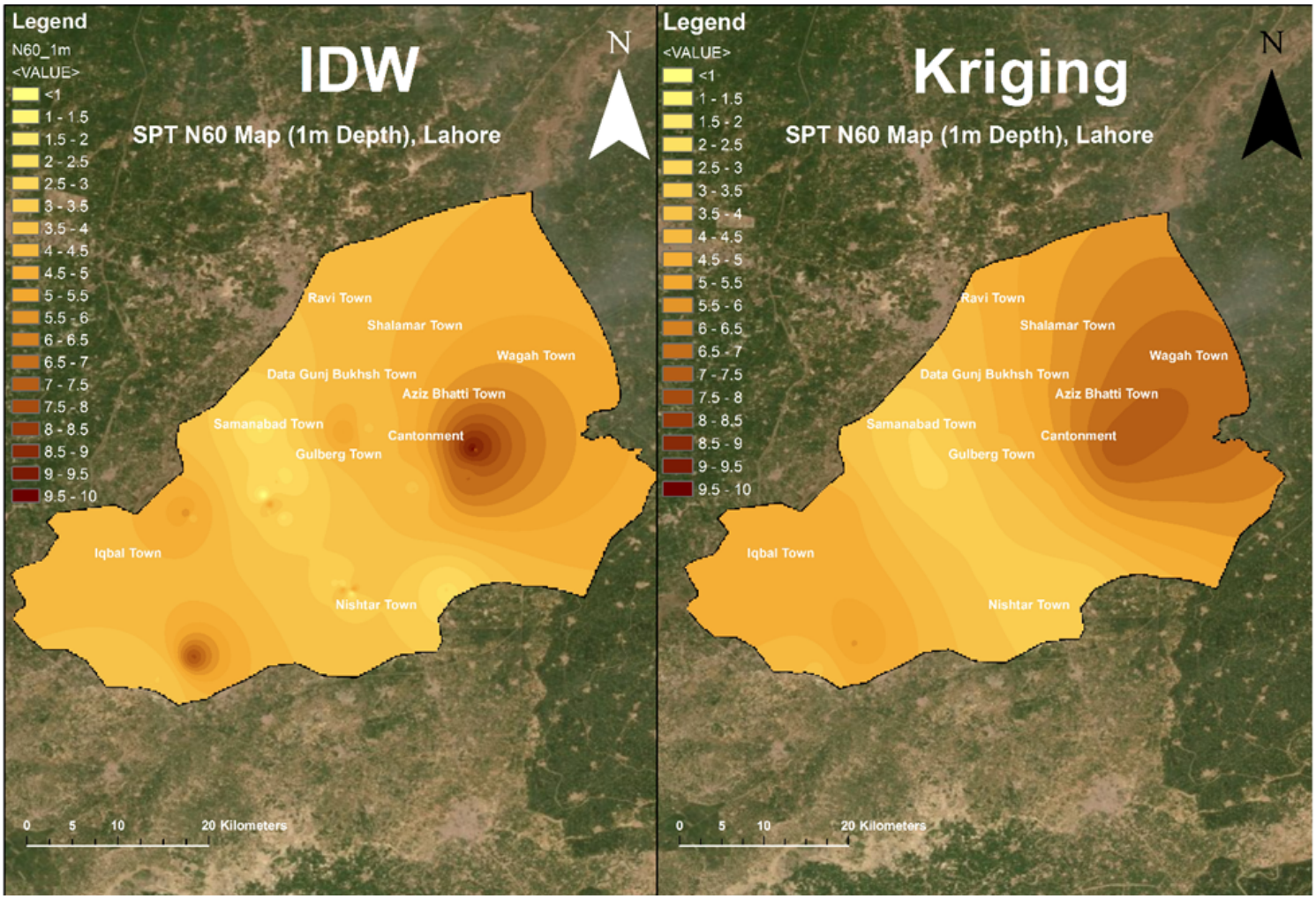

Figure 3

Contour map of SPT N60 (corrected blows or N values) at 1m depth, generated using IDW and Kriging contouring techniques

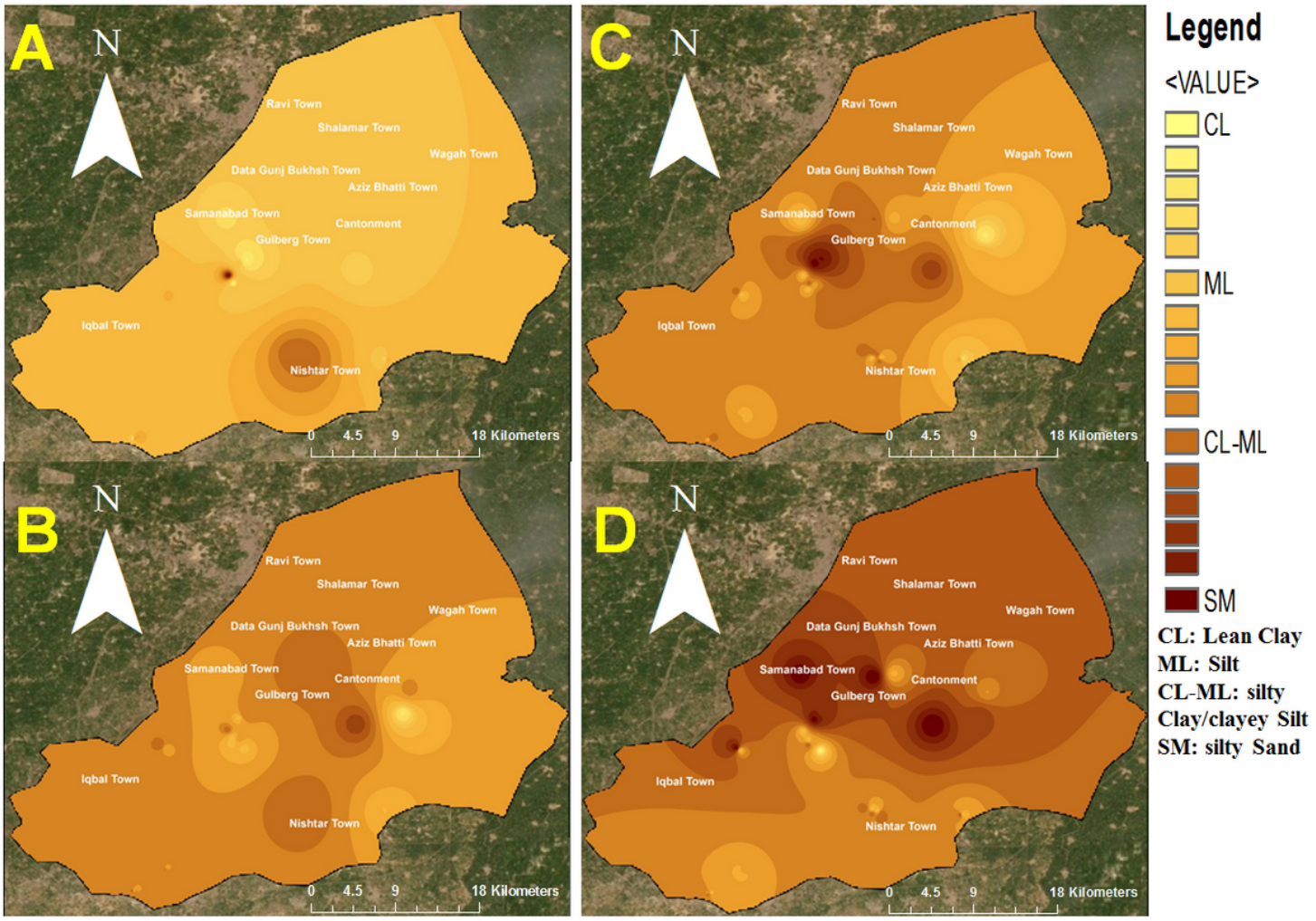

Figure 4

Contour maps of soil types at (A) 1m, (B) 2m, (C) 3m, and (D) 4m depth

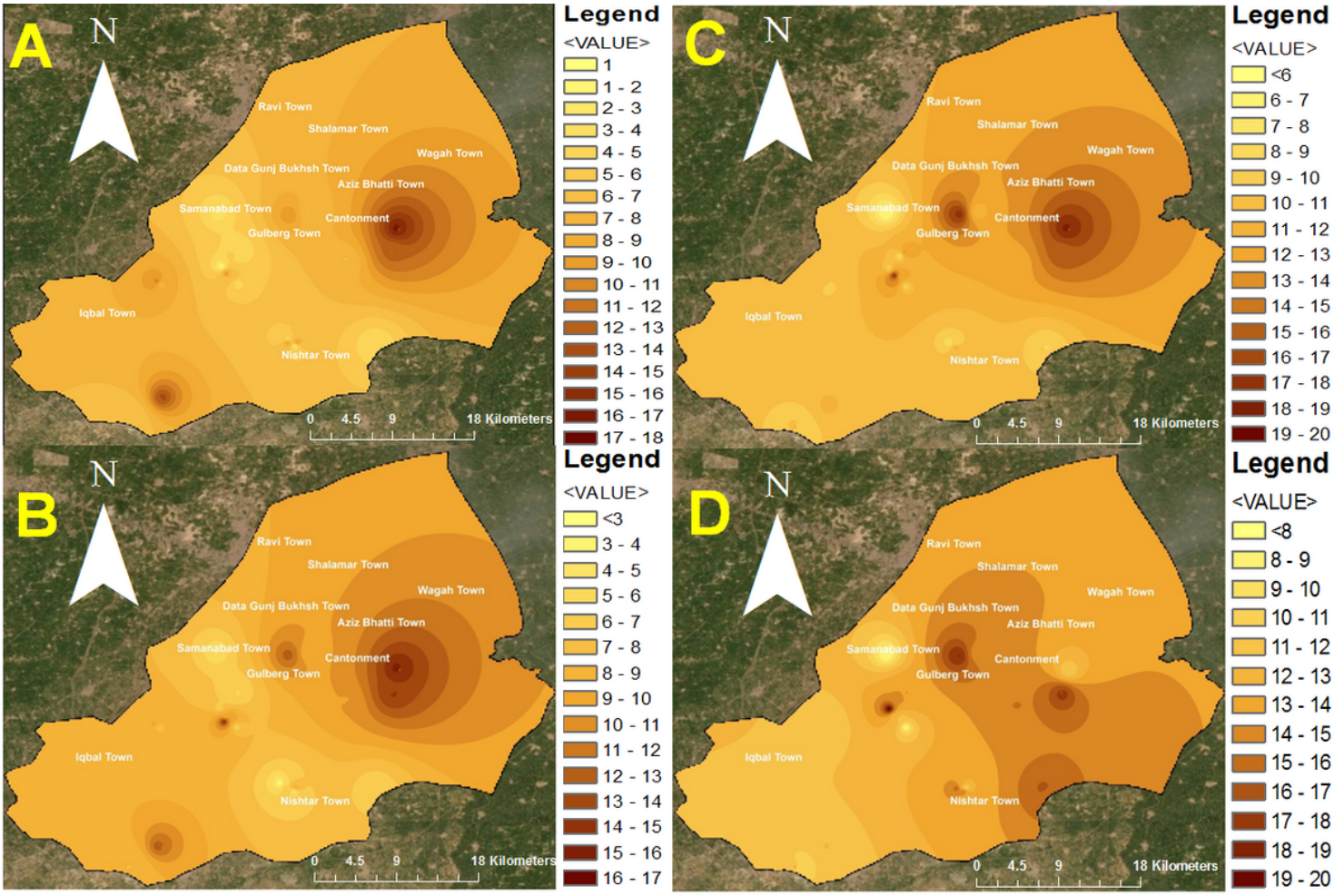

Figure 5

Contour map of SPT N-values at (A) 1m, (B) 2m, (C) 3m, and (D) 4m depth

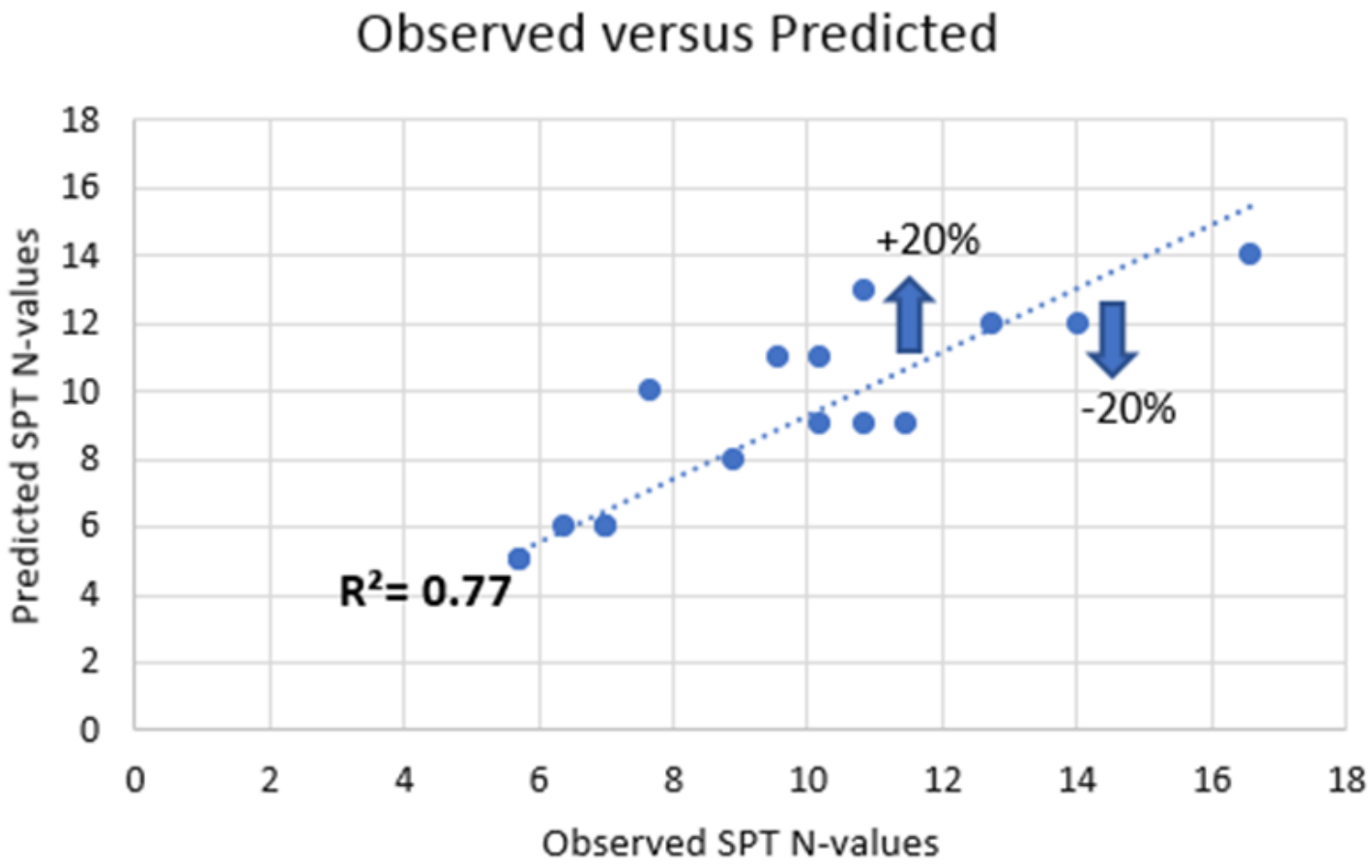

Figure 6

Cross plot of observed (measured in the borehole) and predicted (estimated from the map at the same location) SPT N-values

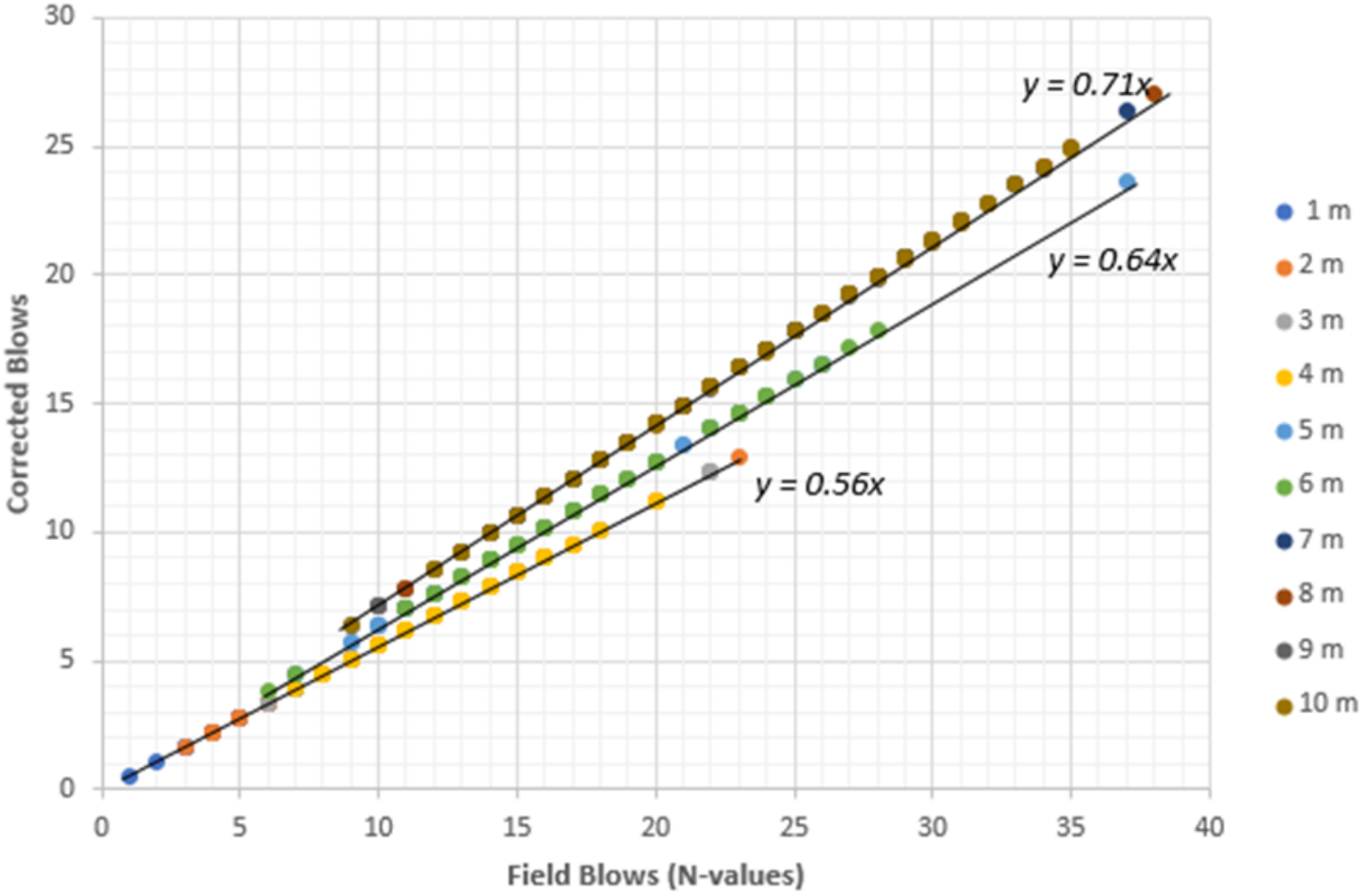

Figure 7

Cross plot between measured (field blows or N values) and corrected blows (N_{60}) of SPT test overlaid with depth

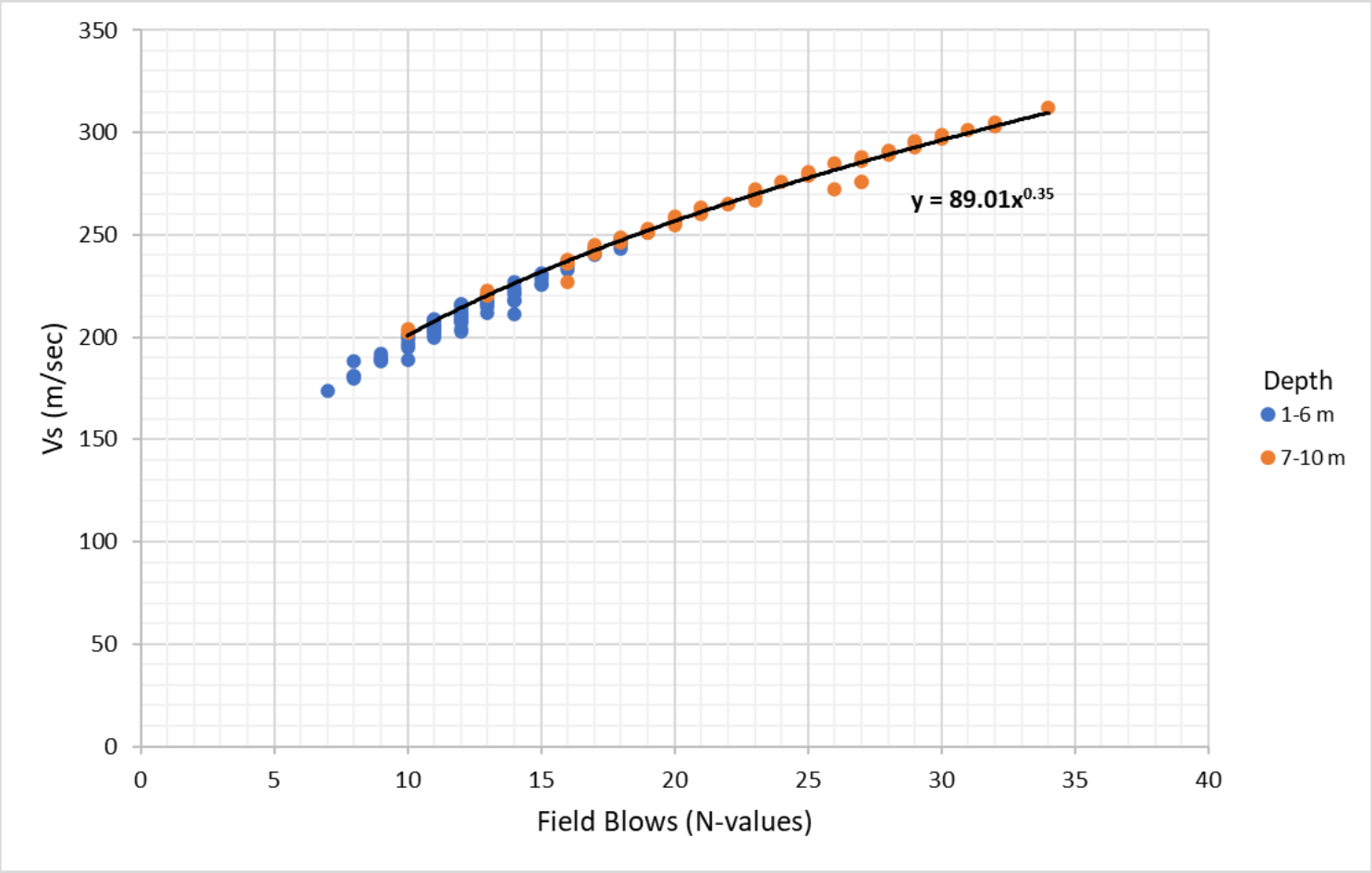

Figure 8

Cross-plot between shear wave velocity & SPT N values color coded with the depth intervals (1-6 m and 7-10 m)

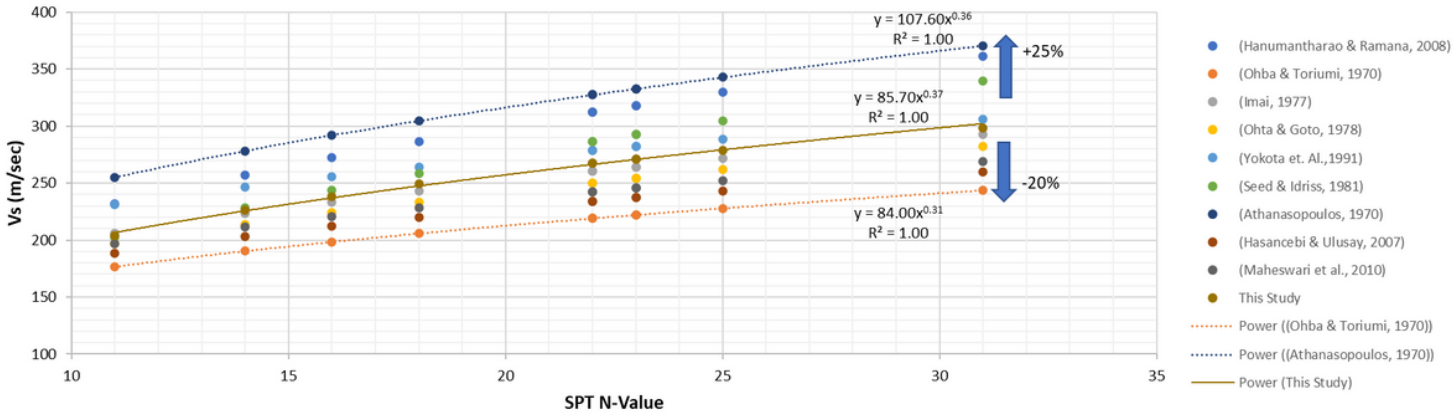

Figure 9

Cross-plot between SPT N-value and Vs, colored points link to different equations given in Table 2

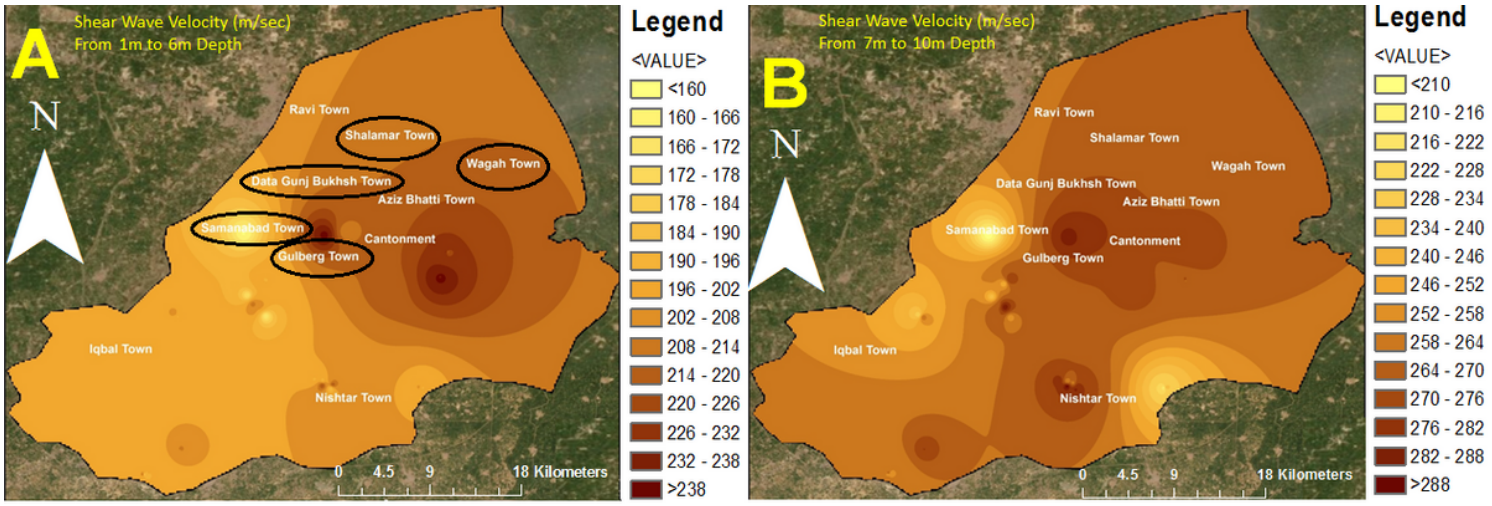

Figure 10

Contour maps of Vs for depth intervals of 1-6 m (A) and 7-10 m (B)

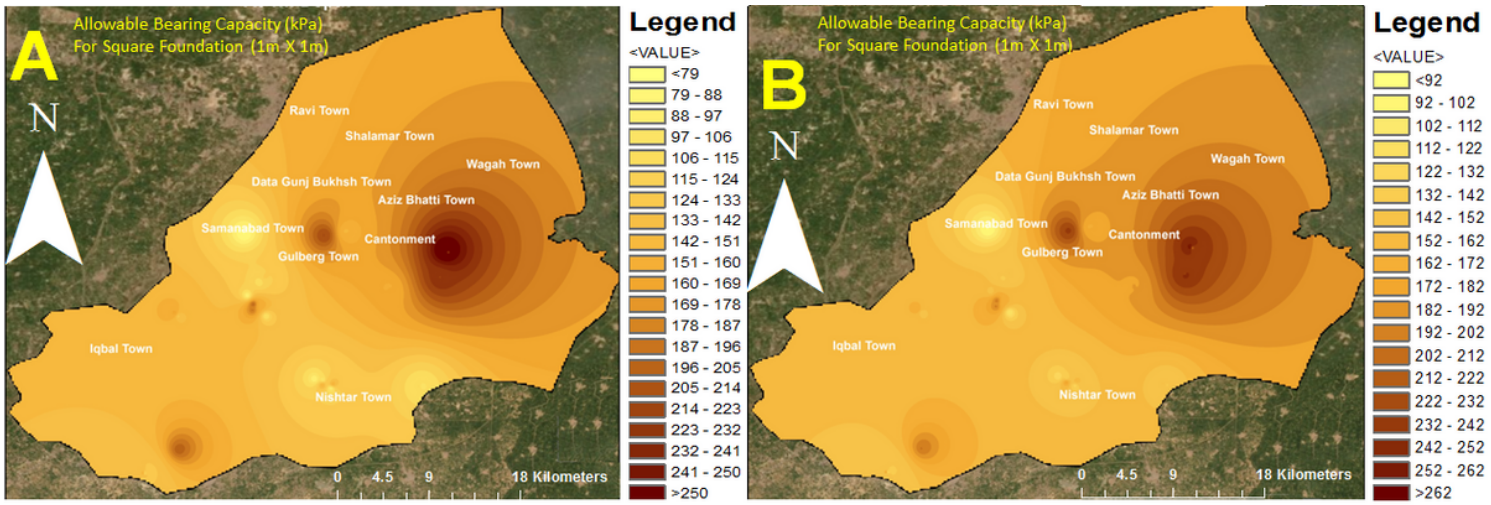

Figure 11

Contour maps of allowable bearing capacity at (A) 1m depth and (B) 2m depth

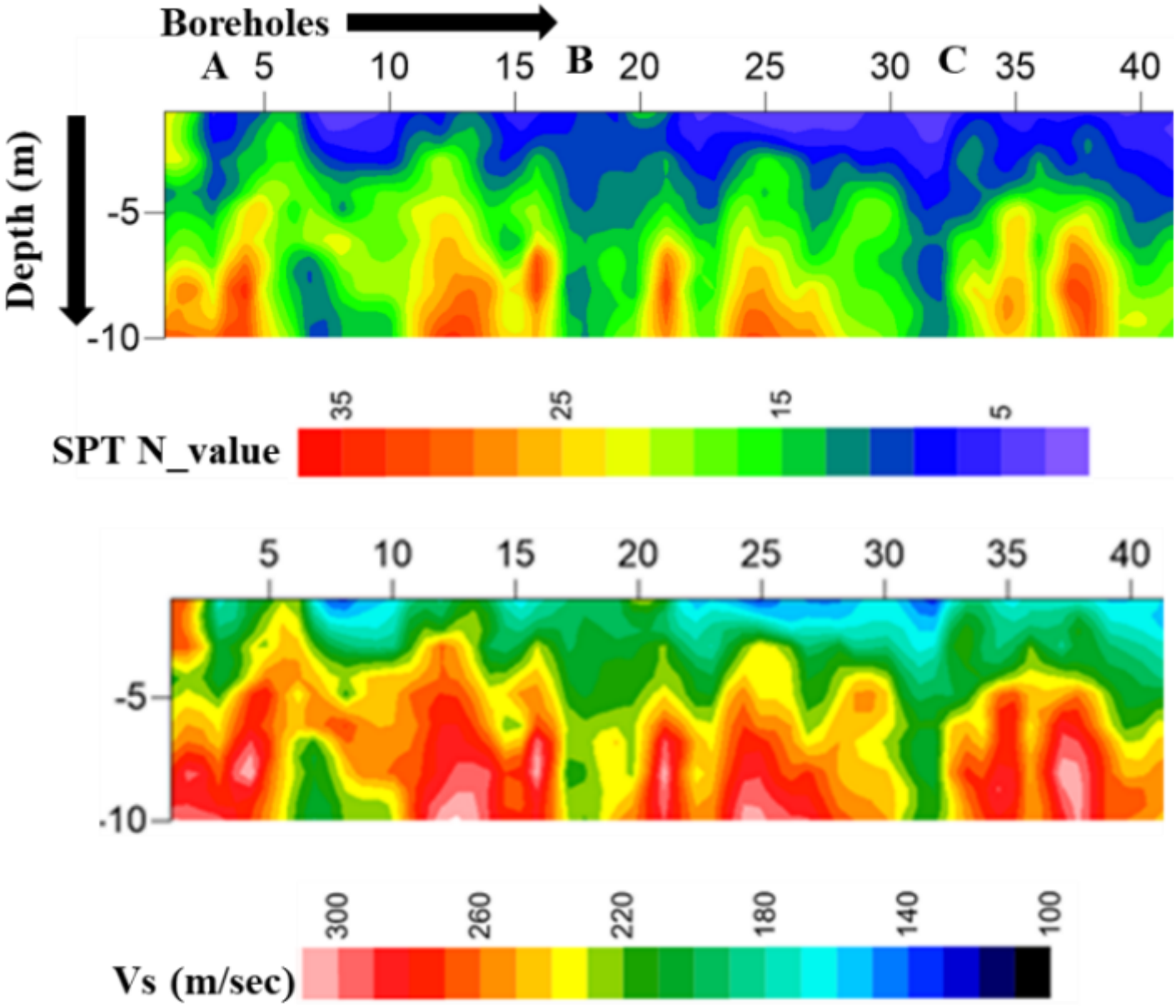

Figure 12

Vertical contour maps of SPT N values & Vs

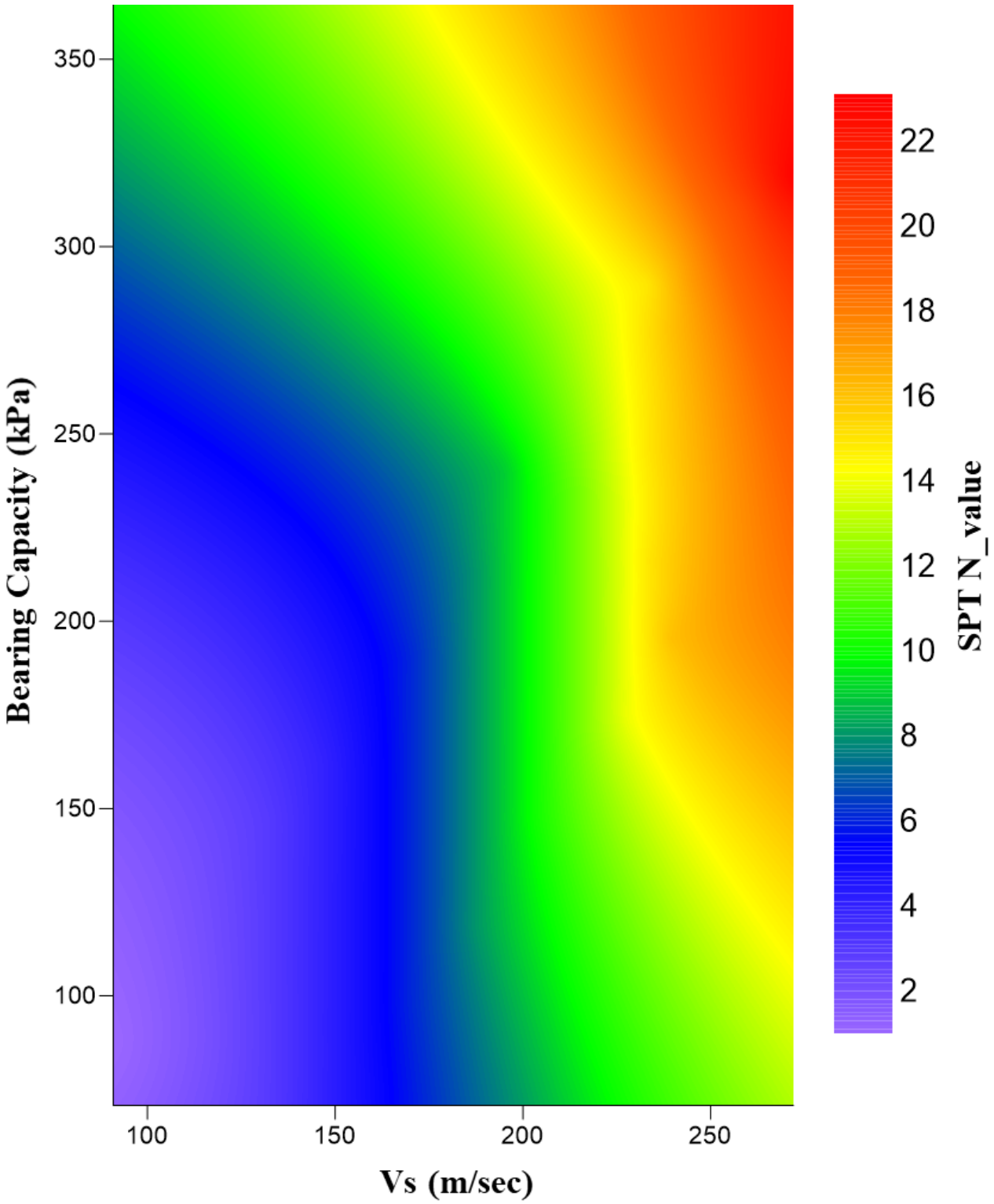

Figure 13

Contour map shows the interrelationship of allowable bearing capacity, Vs, and SPT N values

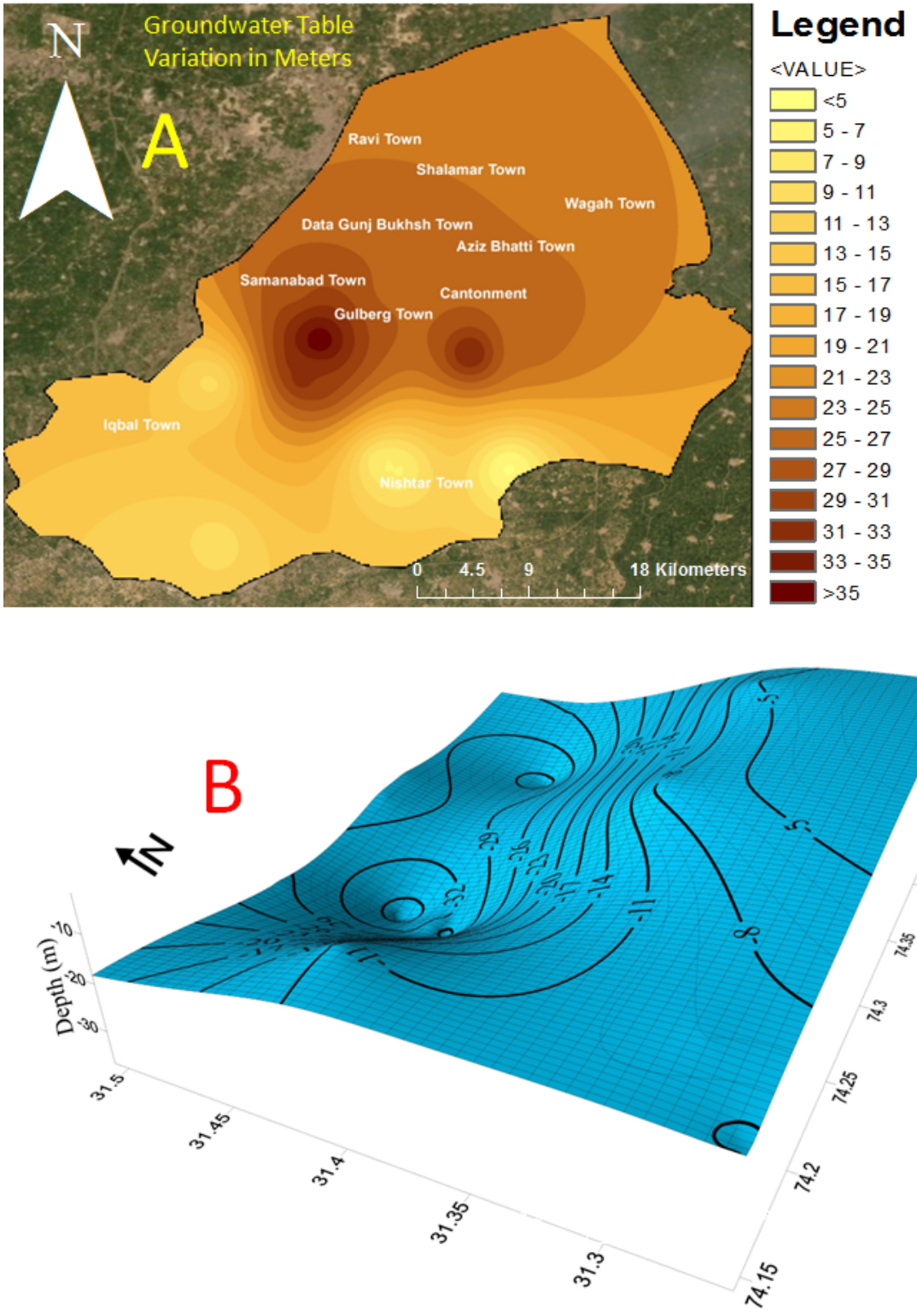

Figure 14

A) Contour map of groundwater table, B) 3D contour map of groundwater table

Supplementary Files

This is a list of supplementary files associated with this preprint. Click to download.

- AppendixSoil.png
- AppendixSPT.png